MOLECULAR MODELING STUDY OF CLAY-BASED NANOCOMPOSITE FILLERS

Jonáš TOKARSKÝ[a,b], Vlastimil MATĚJKA[a]

[a] *NANOTECHNOLOGY CENTRE, VŠB - TECHNICAL UNIVERSITY OF OSTRAVA, 17 .listopadu 15, 708 33 Ostrava - Poruba, Czech Republic, jonas.tokarsky@vsb.cz, vlastimil.matejka@vsb.cz*

[b] *IT4INNOVATIONS CENTRE OF EXCELENCE, VŠB - TECHNICAL UNIVERSITY OF OSTRAVA, 17 .listopadu 15, 708 33 Ostrava - Poruba, Czech Republic, jonas.tokarsky@vsb.cz*

Abstract

Kaolinite and montmorillonite particles decorated with TiO_2 and ZnO nanoparticles are studied at atomistic level using molecular mechanics approach in Materials Studio modeling environment. TiO_2 and ZnO nanoparticles have been prepared having various crystallographic orientations of planes adjacent to the basal surfaces of clays. Mutual nanoparticle-clay interaction energy was calculated and used for a comparison of models of both fillers. Clays can be also used in exfoliated form achieved in this work by the intercalation of urea into the interlayer space. In this part of study, molecular modeling was used as an auxiliary tool and models containing various amount of water and urea molecules in the interlayer space of kaolinite and montmorillonite were prepared. Comparison of data from simulated diffraction analysis of optimized models with experimental data obtained from X-ray powder diffraction analysis of real samples helped to describe the situation in the interlayer space after the intercalation process.

Keywords:

ZnO, TiO_2, urea, clay, molecular modeling

1. INTRODUCTION

Polyamide1010 belongs to the family of thermoplastic polyamides prepared by an interaction of diamine with dicarboxylic acid. Due to its strength, elasticity and toughness, polyamide1010 is used in many practical applications such as transporting pipes, tires, mechanical parts or military equipment [1]. Properties of polyamide1010 can be further enhanced by addition of appropriate fillers [2,3]. Present work, focused on molecular modeling of clay-based nanocomposites, is a part of large project devoted to the comprehensive study of clay-based nano-fillers. Since some informations are difficult to obtain experimentally from real samples, Materials Studio modeling environment was used for obtaining such information as mutual crystallographic orientation of clays and adjacent nanoparticles or amount of urea in the interlayer space of clay after intercalation.

2.1 Preparation and characterization of real samples

Clay/TiO_2 and clay/ZnO composites have been using hydrolysis of $TiOSO_4$ and $ZnCl_2$, respectively, in presence of clay, i.e. either montmorillonite (MMT; d_{001}=9.96 Å) or kaolinite (KLT; d_{001}= 7.16 Å). Size fraction < 40 μm was used. After 3 hours of stirring the composites were filtered, rinsed with distilled water and dried at 70°C. Samples of clays intercalated by urea (U) were prepared by the dry route. Mechanical mixtures (80 wt.% of KLT and 20 wt.% of U, 60 wt.% of MMT and 40 wt.% of U) were heated at 95°C for 24 h. The interlayer distance was measured using Bruker D8 Advance diffractometer (2θ range: 5-50°; $Co_{K\alpha}$ source (λ = 1.78897 Å), Bragg-Brentano geometry). Scanning electron microscope Jeol QUANTA FEG was used for the visual observation of real samples. Images were obtained using a secondary electron detector. Thermogravimetry analysis was performed using SETSYS 18TM thermal analyser. Samples were heated in air atmosphere (heating rate: 10°C min^{-1}; range: 25-1100°C).

2.2 Preparation of initial models

All models have been prepared and optimized in Accelrys Materials Studio/Forcite module modeling environment. Models of NPs (TiO_2, ZnO) and substrates (MMT, KLT) were built separately and then combined into initial models containing substrate and NP adjacent to its surface. Models of MMT ($Al_2Si_4O_{10}(OH)_2$) and KLT ($Al_4Si_4O_{10}(OH)_8$) unit cells have been built using the data published in [4,5,6]. Subsequently, the non-periodic structures of MMT and KLT with the similar size 72 × 54 Å and crystallochemical formulae $(Ca_5K_{12}Na_{36})$ $(Al_{252}Mg_{42}Fe^{3+}_{42})$ $(Si_{654}Al_{18})$ O_{1680} $(OH)_{334}$ and Al_{336} Si_{336} O_{850} $(OH)_{652}$, respectively, have been prepared as the substrates. Both tetrahedral and octahedral surfaces of KLT (denoted as KLT-SiO and KLT-OH) were studied. TiO_2 a ZnO crystal structures were taken from [7] and [8], respectively. Two sets of NPs (six TiO_2 and six ZnO NPs) were built so that their bases (i.e., atomic planes adjacent to the surface of substrate) correspond to the following *hkl* planes: (*001*), (*100*), (*110*). While the bases of NPs from the first triad in both sets contained mainly oxygen atoms (denoted as TiO_2-O and ZnO-O) the bases of NPs from the second triad contained mainly metal atoms (denoted as TiO_2-Ti and ZnO-Zn). It was thus possible to monitor the influence of crystallographic orientation and type of atoms on the mutual NP-substrate interaction. Interaction energy (E_{int}) was calculated using the following equation

$$E_{\text{int}} = \frac{E_{tot} - (E_{tot,NP} + E_{tot,sub})}{S} \quad (1)$$

where E_{tot} is the total potential energy of model (i.e., NP+substrate), $E_{tot,NP}$ is the total potential energy of NP and $E_{tot,sub}$ is the total potential energy of substrate. S is the surface area of NP's plane adjacent to the substrate. Therefore, the E_{int} is expressed in kcal mol^{-1} $Å^{-2}$. The lower value the stronger interaction between NP and substrate.

Models of the MMT and KLT interlayer space were built under the periodic boundary conditions. Using the data published in [4,5] the supercell structure of MMT having crystallochemical formula $(Ca^{2+}_4K^{+}_2Na^{+}_6)$ $(Al_{42}Mg_7Fe^{3+}_7)$ $(Si_{109}$ $Al_3)$ O_{280} $(OH)_{56}$ and cell parameters a = 36.358 Å, b = 17.992 Å, c = 30.494 Å (double value compared to [4]), α = 90.00°, β = 95.18°, γ = 90.00° was prepared. KLT supercell Al_{32} Si_{32} O_{80} $(OH)_{64}$ was prepared according to [6]. Cell parameters were a = 20.596 Å, b = 17.868 Å, c = 14.768 Å (double value compared to [6]), α = 91.93°, β = 105.04°, γ = 89.79°. Models of the KLT and MMT interlayer space contained various amounts of U and water (W) molecules. Lattice parameters a, b and γ were fixed during geometry optimization procedure. Charges of atoms in NPs and clays were assigned using QEq method [9] while for charges of U and W the Gasteiger method was used [10]. All models have been optimized using Universal force field [11]. A Smart algorithm was used for the geometry optimization with 100 000 iteration steps. In order to monitor the changes of d_{001} value in dependence on the interlayer content, simulated diffraction patterns have been calculated for each optimized model in Materials Studio/Reflex module under the same conditions as in the experiment (i.e., 2θ range: 5-50°; $Co_{K\alpha}$ irradiation (λ = 1.78897 Å), Bragg-Brentano geometry).

3. RESULTS AND DISCUSSION

3.1 Nanoparticle-clay interaction

Mutual NP/substrate interaction energies calculated from optimized models are listed in Table 1. These results show that NPs adhere to the MMT and KLT-SiO surfaces preferentially via O atoms while in case of KLT-OH surface the NPs prefer to be adjacent via Zn or Ti atoms and the interaction is weaker. Therefore, MMT can be considered as a substrate on which the more complete coverage by NPs can be expected. ZnO NPs generally exhibit lower E_{int} values that TiO_2 NPs and KLT-OH surface seems to be very unsuitable for their anchoring. Only one ZnO/KLT-OH model successfully converged to the energetical minimum while for others the minima were found only when NPs were very far (in order of nm) from the KLT-OH surface. These results were confirmed by SEM analyses showing much more complete coverage of clay surface by TiO_2

NPs than by ZnO NPs (Fig. 1). Table 1 also shows differences between E_{int} values for various hkl planes. In case of ZnO the preferred orientation is the same for all substrates, i.e., ZnO(001) plane is preferred. TiO_2 NPs adhere by (001) plane only to KLT surfaces and in TiO_2/MMT models the (100) plane is preferred.

Table 1. Interaction energies between NPs and surfaces of MMT and KLT. NPs adhere via either oxygen (TiO_2-O, ZnO-O) or metal (TiO_2-Ti, ZnO-Zn) atoms. Both tetrahedral (KLT-SiO) and octahedral (KLT-OH) surfaces of KLT are taken into account. S [nm^2] is the surface area of hkl plane adjacent to the substrate.

hkl	S [nm^2]	E_{int} [kcal · mol^{-1} · nm^{-2}]					
		TiO_2-O			TiO_2-Ti		
		MMT	KLT-SiO	KLT-OH	MMT	KLT-SiO	KLT-OH
001	1.526	-2615	-2562	-1952	-2471	-2425	-2301
100	1.315	-3048	-2286	-2076	-2850	-2208	-2282
110	1.766	-2189	-1623	-1690	-2138	-1490	-1999
hkl	**S [nm^2]**	**E_{int} [kcal · mol^{-1} · nm^{-2}]**					
		ZnO-O			**ZnO-Zn**		
		MMT	**KLT-SiO**	**KLT-OH**	**MMT**	**KLT-SiO**	**KLT-OH**
001	1.914	-2026	-1568	-	-1946	-1331	-329
100	2.642	-1326	-1036	-	-1284	-897	-247
110	2.777	-526	-394	-	-434	-336	-

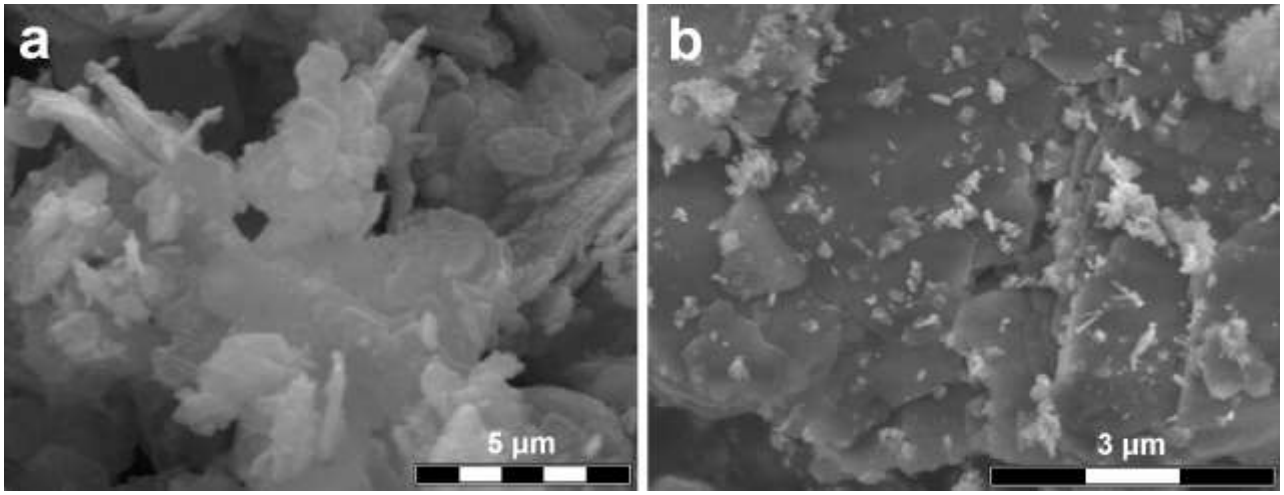

Fig. 1. SEM images of (a) TiO_2/KLT and(b) ZnO/KLT nanocomposites. Large uncovered areas of KLT surface in case of ZnO/KLT sample can be seen.

3.2 Water and urea in the interlayer space

Various models of MMT and KLT interlayer space with different amount of U and W molecules were optimized and their computed d_{001} values were compared with d_{001} values of real samples. Fig. 2a clearly shows that the experimentally obtained value d_{001} ~ 16.9 Å of real MMT sample agrees well with three MMT models containing 10.20 wt.% and 15.29 wt.% (d_{001}=16.82 Å; Fig. 3a), 16.71 wt.% and 10.30 wt.% (d_{001}=17.13 Å; Fig. 3b), and 21.06 wt.% and 5.05 wt.% (d_{001}=16.96 Å; Fig. 3c) of U and W, respectively. Real KLT sample has d_{001} ~ 10.7 Å and the good agreement was obtained in case of KLT models containing 2.37 wt.% and 16.01 wt.% (d_{001}=10.68 Å; Fig. 3d), 11.62 wt.% and 8.37 wt.% (d_{001}=10.76 Å; Fig. 3e), and 14.01 wt.% and 5.61 wt.% (d_{001}=10.75 Å; Fig. 3f) of U and W, respectively.

Three MMT models having d_{001} values close to the experimental value 16.9 Å are shown in Figs. 3a-c. It can be clearly seen that U molecules in the MMT interlayer space are arranged so that C=O functional groups (bearing a negative partial charge) are oriented to the center of the interlayer space while positively charged NH_2 groups are oriented toward the negatively charged MMT layers. W molecules are distributed homogeneously in all MMT models and coordinate the interlayer cations. In the model with 10.20 wt.% of U

(Fig. 3a) the U molecules appear to organize into two layers. Higher amount of U (16.71 wt.%) allows the formation of two distinct layers (Fig. 3b) and in the case of even higher amount (21.06 wt.%) a third layer seems to be formed (Fig. 3c).

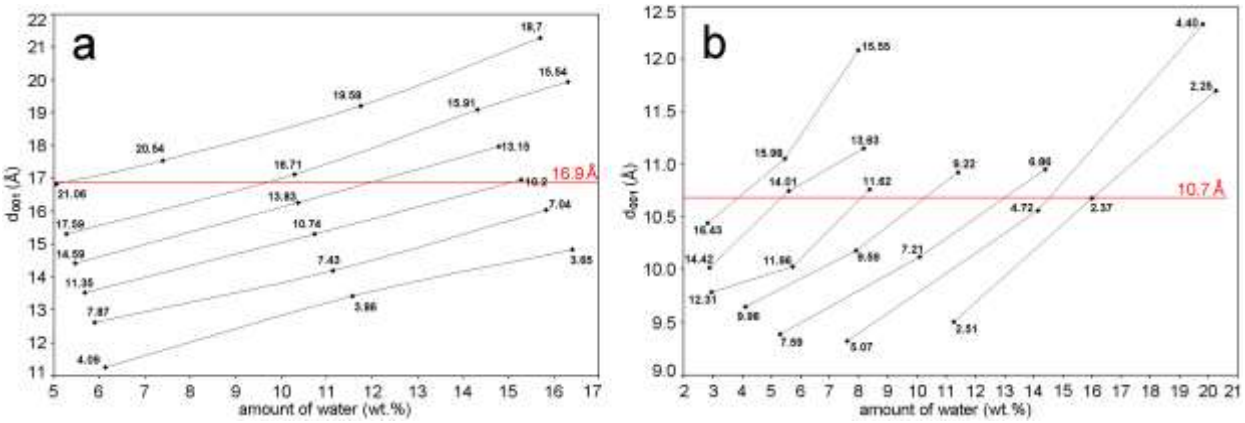

Fig. 2. Dependence of computed d_{001} values on amount of water (x axis) and amount of urea (points) in models of the MMT (a) and KLT(b) interlayer space. Experimental d_{001} values obtained from real samples are shown in red.

Three KLT models having d_{001} values close to the experimental value 10.7 Å are shown in Figs. 3d-f and it can be seen that the arrangement of U and W molecules differs from the arrangement in MMT. KLT contains lower amount of U and the orientation is affected by the type of KLT layers. With the increasing amount of U the increasing number of molecules oriented by the C=O group toward the tetrahedral sheet can be observed (compare Figs. 3d, 3e, 3f). Moreover, the lower amount of W molecules the higher portion of them can be found near the octahedral sheet.

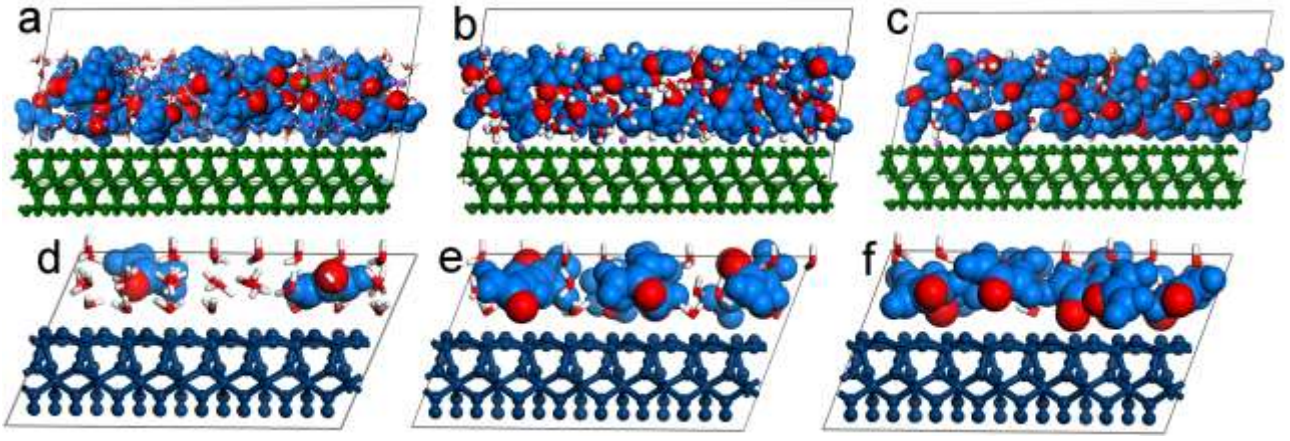

Fig. 3. Optimized models of the MMT (a-c) and KLT (d-f) interlayer space. Models having d_{001} values 16.82 Å (a), 17.13 Å (b), 16.96 Å (c), 10.68 Å (d), 10.76 Å (e), and 10.75 Å (f) are shown. Urea molecules are blue, oxygens in urea are red.

As mentioned before, total weights of U and W molecules in the interlayer space are nearly constant for given d_{001} values and the content of the MMT and KLT interlayer space represents ~19 and ~26 wt.% of the model, respectively. This finding is in good agreement with results of TG analysis where for the KLT/urea sample the weight loss ~18 wt.% was observed in temperature range 150-400°C. Optimized models of KLT interlayer space containing only W molecules showed that pristine KLT having d_{001}= 7.16 Å has 4.2 wt.% of W in the interlayer space. Taking into account that KLT/urea was prepared by the dry route, the amount of W in the resulting material can be considered approximately the same or slightly lower (heating at 95°C for 24

h) and, therefore, amount of U in the interlayer space cannot be lower than 14 wt.%. Since the initial mixture contained 20 wt.% of U, the intercalation efficiency is about 70 %.

For the MMT/urea sample the weight loss was ~20 wt.% in the range 150-300°C. The amount of U and W calculated from optimized models is higher (~26 wt.%) but taking into account the Coulombic interactions between U and negatively charged MMT layers it is probable that the loss of U occurs also at the temperature range 300-1000°C at which, however, also the dehydroxylation of MMT structure begins. These two processes are difficult to separate from each other and decrease in weight of the sample may be caused by both of them. Optimized models of MMT interlayer space containing only W molecules showed that pristine MMT having d_{001}= 9.96 Å has 3.3 wt.% of W in the interlayer space and because of preparation of the MMT/urea sample by the dry route the amount of W in the resulting material can be considered approximately the same or slightly lower (as same as in the case of KLT/urea). The amount of U can be easily calculated from obtained results. Using formula describing the dependence of number of U on the number of W in the MMT interlayer space for d_{001}~ 16.9 Å (Fig. 4) the amount of U is 23.43 wt.% for 3.3 wt.% of W and even higher for lower amount of W. Since the initial mixture contained 40 wt.% of U, the intercalation efficiency is about 60%. This lower intercalation efficiency can be explained by the presence of interlayer cations forming a barrier to prevent easy intercalation of U molecules into the MMT interlayer space.

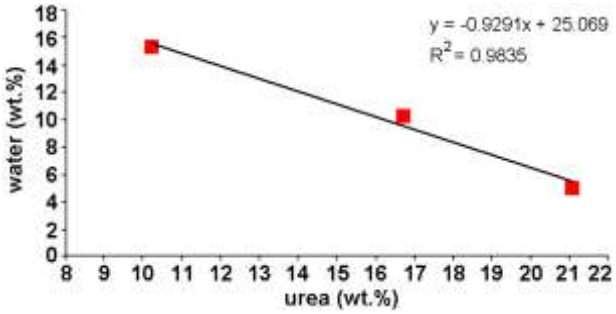

Fig. 4. The dependence of number of urea molecules on the number of water molecules in the MMT interlayer space for d_{001}~ 16.9 Å.

4. CONCLUSIONS

Molecular modeling was used as a tool for the characterization of clay-based materials containing TiO_2 and ZnO nanoparticles on the surface and urea and water molecules in the interlayer space. It was found that nanoparticles adhere to the MMT and KLT-SiO surfaces preferentially via oxygen atoms and to the KLT-OH surface via metal atoms which results in the weaker interaction. Preferred crystallographical orientation of ZnO nanoparticles is (001) for all substrates while TiO_2 nanoparticles adhere by (001) plane to KLT surfaces and by (100) plane to the MMT.

Regarding the clay/urea intercalates, molecular modeling proved to be a useful tool for determining the amount of molecules in the interlayer space of clays. Calculated values are in good agreement with available experimental data and, therefore, our molecular modeling approach can be used for other similar studies of clay-based materials.

ACKNOWLEDGEMENT

This work was supported by the Ministry of Education, Youth and Sports of Czech Republic project (LH12184) and by the European Regional Development Fund in the IT4Innovations Centre of Excellence project (CZ.1.05/1.1.00/02.0070). Authors thank K. Dědková and B. Smetana for SEM and TG analyses.

REFERENCES

[1] MO, Z., MENG, Q., FENG, J., ZHANG, H., CHEN, D. Crystal structure and thermodynamic parameters of Nylon-1010, *Polymer International*, 1993, vol. 32, iss. 1, p. 53-60.

[2] KOJIMA, Y., USUKI, A., KAWASUMI, M., OKADA, A., KURAUCHI, T., KAMIGAITO, O., Synthesis of nylon 6-clay hybrid by montmorillonite intercalated with ε-caprolactam, *Journal of Polymer Science A*, 1993, vol. 31, iss. 4, p. 983-986.

[3] CHIU, C.W., HUANG, T.K., WANG, Y.C., ALAMANI, B.G., LIN, J.J., Intercalation strategies in clays/polymer hybrids*, Progress in Polymer Science*, 2014, vol. 39, iss. 3, p. 443-485.

[4] TSIPURSKI, S.I., DRITS, V.A. The distribution of octahedral cations in the 2:1 layers of dioctahedral smectites studied by oblique-texture electron diffraction, *Clay Minerals*, 1984, vol. 19, iss. 2, p. 177-193.

[5] MÉRING, J., OBERLIN, A. Electron-optical study of smectites, *Clays and Clay Minerals*, 1967, vol. 15, iss. 1, p. 3-25.

[6] NEDER, R.B., BURGHAMMER, M., GRASL, T., SCHULTZ, H., BRAM, A., FIEDLER, S. Refinement of the kaolinite structure from single-crystal synchrotron data, *Clays and Clay Minerals*, 1999, vol. 47, iss. 4, p. 487-494.

[7] HOWARD, C.J., SABINE, T.M., DICKSON, F. Structural and thermal parameters for rutile and anatase, *Acta Crystallographica B*, 1991, vol. 47, iss. 4, p. 462-468.

[8] R.W.G. WYCKOFF: Crystal Structures, Vol.1, John Wiley & Sons, New York, 1963, p. 110-112.

[9] RAPPÉ, A.K., GODDARD, W.A. Charge equilibration for molecular dynamics simulations, *Journal of Physical Chemistry*, 1991, vol. 95, iss. 8, p. 3358-3363.

[10] GASTEIGER, J., MARSILI, M. Iterative partial equalization of orbital electronegativity: a rapid access to atomic charges, Tetrahedron, 1980, vol. 36, iss. 22, p. 3219-3228.

[11] RAPPÉ, A.K., CASEWIT, C.J., COLWELL, K.S., GODDARD, W.A., SKIFF, W.M. UFF, a full periodic table force field for molecular mechanics and molecular dynamics simulations, *Journal of American Chemical Society*, 1992, vol. 114, iss. 25., p. 10024-10035.